Design and Economic Trade-Offs of Extractive Crystallization Processes

Shankar Rajagopal, Ka M. Ng, and James M. Douglas
Dept. of Chemical Engineering, University of Massachusetts, Amherst, MA 01003

A systematic procedure is formulated for the separation of a binary mixture by means of extractive crystallization. It shous that two flowsheet structures can handle systems with a wide variety of solid-liquid phase behaviors, including components with simple eutectics, multiple eutectics, and compound formation. Design equations are presented for both flowsheet structures. In addition, design variables and constraints are identified. The economic trade-offs in extractive crystallization processes are examined through the analysis of an example: the complete separation of para-xylene from meta-xylene using n-pentane as the extractive solvent. Comparison of our general methodology with the system-specific designs reported in the literature shows that the latter are process alternatives of the former.

Introduction

Crystallization has been used for separating components from each other for a long time in the chemical process industry. One important problem in the complete separation of a binary mixture by means of crystallization is caused by the presence of one or more eutectics. Since both components crystallize out at the eutectic composition, the maximum recovery of a pure component is limited by the eutectic point. Two important methods have been used to overcome this limitation imposed by eutectics. These are adductive and extractive crystallization processes. Comprehensive discussions of these processes are available (Findlay and Weedman, 1958; Findlay, 1962; Dale, 1981).

In adductive crystallization, an adduct—a crystalline solid phase—is formed by adding a third component to the mixture. This chosen agent should form an adduct with one of the components in a selective manner. The adduct formed is subsequently separated and then dissociated, usually by means of heat, to recover the component from the extraneous component. McCandless et al. (1972, 1974) used thiourea as the adduct-forming compound in the separation of trimethylpentanes and in the separation of *para*-xylene from ethylbenzene. Dewaxing of oil using urea adducts has been a successful commercial process (Brenken and Richter, 1979).

In extractive crystallization, a third component is also added to the two components to modify the solid-liquid phase behavior. This extraneous agent does not form a solid phase at any point in the process. We will discuss in detail how a binary mixture is completely separated. Findlay et al. (1958) describe in detail an extractive crystallization process in which *para*-xylene and *meta*-xylene are completely separated from each other by using *n*-heptane as the extractive solvent. Extractive crystallization was used to separate *meta* and *para* cresols (Chivate and Shah, 1956), and *ortho* and *para* nitrochlorobenzenes (Dikshit and Chivate, 1970; Tare and Chivate, 1976). An advantage of extractive crystallization over adductive crystallization is that the components are crystallized in their pure forms, eliminating the need for separating an adduct. We will focus on extractive crystallization in this paper.

The conventional extractive crystallization process described in the literature is system specific and it is not clear how to separate any given system in a general way. There has been very little work on the identification of other possible alternative flowsheets. Thus, the primary objective of this study is to formulate a general methodology for using extractive crystallization as a tool for the complete separation of any two components. The conventional extractive crystallization described in detail by Findlay and Weedman (1958) uses three crystallizers and three filters, while the general methodology we propose below needs only two crystallizers and two filters. The secondary objective is to identify the key design variables and to evaluate the economics of extractive crystallization processes. Very little discussion on process economics is available

Correspondence concerning this article should be addressed to K. M. Ng.
The current address of S. Rajagopal is Amoco Chemical Company, P. O. Box 400, Naperville, IL 60566.

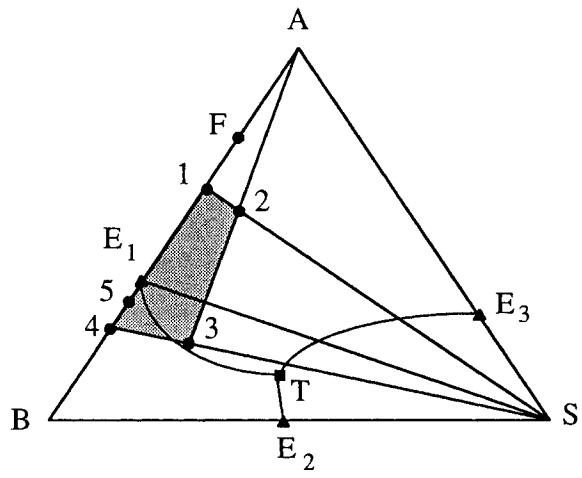

Figure 1. Solid-liquid phase diagram of type I flowsheet for components *A* and *B*.

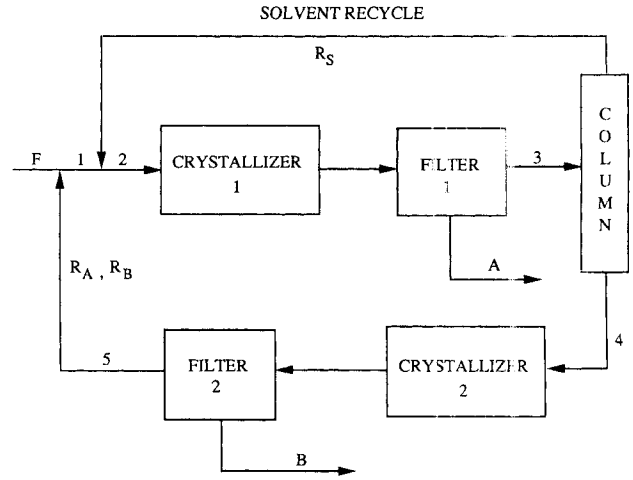

Figure 2. Type I extractive crystallization flowsheet.

in the literature. With a general methodology and a better understanding of process economic trade-offs, the design engineer is in a better position to apply this process to the problem of separating any given binary mixture.

We begin with a description of the general procedure for simple eutectic systems. For a two-component system and an extractive agent, we have three binary eutectics and one ternary eutectic, and these components do not combine to form different compounds (Mullin, 1972). The general methodology is then applied to systems with more complex phase behavior. Next, the design equations are presented and the key design variables are identified. This is followed by a case study of the separation of *para* and *meta* xylenes, providing a better understanding of the optimization of an extractive crystallization process. Finally, we show that the conventional scheme is simply a process alternative of the general method.

General Methodology

A ternary diagram of the solid-liquid phase behavior for a three-component system with simple eutectics is shown in Figure 1. This phase diagram will be referred to as type I. Components A and B are the two components to be separated and the feed composition is represented in the phase diagram by the point F. The extractive solvent is represented by the vertex S. The binary eutectic points are represented by E_1, E_2, and E_3 and the ternary eutectic point is represented by T. The appropriate flowsheet structure for this phase diagram is shown in Figure 2. The compositions of the liquid phase in various streams of the process are indicated by numbers in the flowsheet as well as in the phase diagram. R_A, R_B, and R_S are the recycle molar flow rates of components A, B, and the solvent, respectively. The liquid phase compositions in the process at various points in the flowsheet lie within the shaded area *1234* in Figure 1.

Let us now go through the flowsheet, Figure 2, in detail. The feed mixture of A and B, represented by F, joins a recycle stream of A and B represented by *5*. The composition of the mixed stream is represented by *1* in the phase diagram. Recycled solvent from the solvent recovery column is added to stream *1* to yield stream *2*, which is the feed stream to the first crystallizer. The crystallizer temperature is maintained at T_{C1} and pure component A is crystallized. The composition of the mother liquor from the crystallizer moves down to point *3* in the phase diagram. The mother liquor is separated from the crystals in filter *1* and is the feed stream to the solvent recovery column. Pure solvent is separated from A and B by distillation, and the bottoms composition is represented by point *4* in the phase diagram. It is important to note that the use of distillation to separate the solvent effectively allows us to cross the eutectic trough E_1T. Stream *4* is the feed to crystallizer *2*, where the temperature is maintained at T_{C2}. Component B is crystallized and the composition of the mother liquor moves to point *5* in the phase diagram. The crystals are separated from the mother liquor in filter *2*. The mother liquor from the second crystallizer contains components A and B. It is recycled back to the first crystallizer, where it meets the fresh feed F, to give stream *1*. As will be seen in the design equations to be discussed, the amounts of components A and B crystallized in the two crystallizers can be exactly matched to the amounts in the feed stream by manipulating the recycle flow rates of the solvent, component A, and component B, and the two crystallizer temperatures. In the discussion above, only one temperature is assigned to a crystallizer. Since the temperature might not be uniform in a commercial unit, the temperature at the exit of the crystallizer should be used.

A type II solid-liquid phase diagram is shown in Figure 3 and the corresponding flowsheet is illustrated in Figure 4. The main difference between types I and II phase diagrams is that, in Figure 1, the feed point F and the eutectic trough, joining E_1 with T, are on the opposite sides of the line E_1S, while in Figure 3 they are on the same side. Note that in the case of type II, the recycled solvent is added to the feed stream of the second crystallizer, Figure 4, instead of the first crystallizer, as we have seen in type I, Figure 2.

Let us now go through the flowsheet in Figure 4 in detail. The feed stream is represented by F, and is mixed with a recycle stream from the solvent recovery column, represented by point *5*, to give stream *1*. This stream is fed to the first crystallizer, where the temperature is maintained at T_{C1}, and pure component A is crystallized. Filter *1* is used to separate the crystals from the mother liquor. The mother liquor, represented by *2*, is mixed with the recycled solvent from the solvent recovery

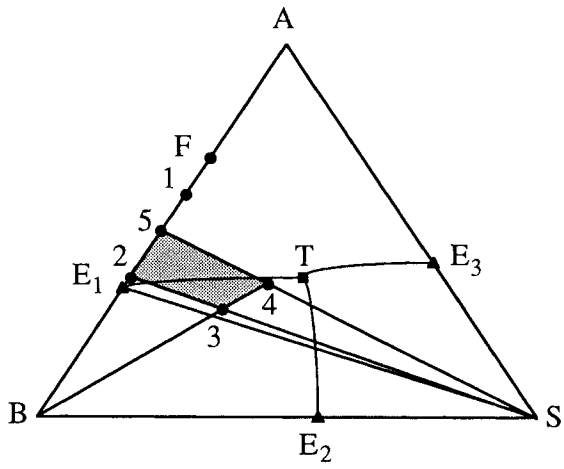

Figure 3. Solid-liquid phase diagram of type II flowsheet for components *A* and *B*.

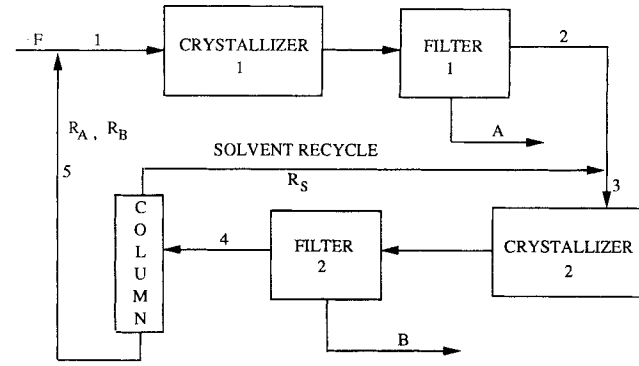

Figure 4. Type II extractive crystallization flowsheet.

column. The composition of the mixed stream is denoted as point *3* in the phase diagram. The mixed stream is the feed to the second crystallizer, where the temperature is maintained at T_{C2}, and component *B* is crystallized. The crystals are separated from the mother liquor using filter *2*. The composition of the mother liquor is represented by point *4* in the phase diagram. The mother liquor is the feed stream to the solvent recovery column, where the solvent is separated from components *A* and *B* and is recycled back to the second crystallizer. Components *A* and *B* from the solvent recovery column, represented by point *5*, are recycled back to the first crystallizer. The liquid phase compositions in the process at various points in the flowsheet lie within the shaded area *2345* in Figure 3.

The two flowsheet schemes can be used to separate any two components with a variety of solid-liquid phase behaviors. For example, in Figure 5 we can see two different hypothetical solid-liquid phase diagrams, in both of which the eutectic trough E_1T intersects the line E_1S at point *X*. As indicated by the shaded areas, Figure 5a uses the type I flowsheet and Figure 5b uses the type II alternative. However, we note that due to this intersection either flowsheet can indeed be used for both phase diagrams. Consider Figure 5a. The shaded area representing type II flowsheet scheme *2345* (see Figure 3 or 5b) can be fitted into the phase diagram as long as points *3* and *4* lie within the triangle formed by *X*, *T*, and the intersection between E_2T and *SX*. Similar arguments can be made for Figure 5b.

The above two sequences can also be used effectively to separate components of industrial importance but with complex solid-liquid phase behaviors. For example, in Figure 6a, we illustrate a way to use the type I sequence to separate *para*-nitrochlorobenzene from its *ortho* isomer using *para*-dibromobenzene as the solvent. There are four binary eutectics and two ternary eutectics. Note that in this figure, as well as Figure 6b, the relative positions of the eutectics are correctly indicated but this phase diagram is not very exact. Tare and Chivate (1976) used a conventional extractive crystallization to separate this system, which requires three crystallizers and three filters. With the type I sequence as indicated by the shaded area, only two crystallizers and two filters are required. Similarly, in Figure 6b, we use the type II sequence to separate *para*-xylene from *meta*-xylene using carbon tetrachloride as the extractive solvent. Again, the problems of compound formation and multiple eutectics do not pose any difficulty provided that the shaded area *2345* is appropriately placed. Egan and Luthy (1955) studied the same system of components. Their proposed process is not based on extractive crystallization and does not recover the components completely.

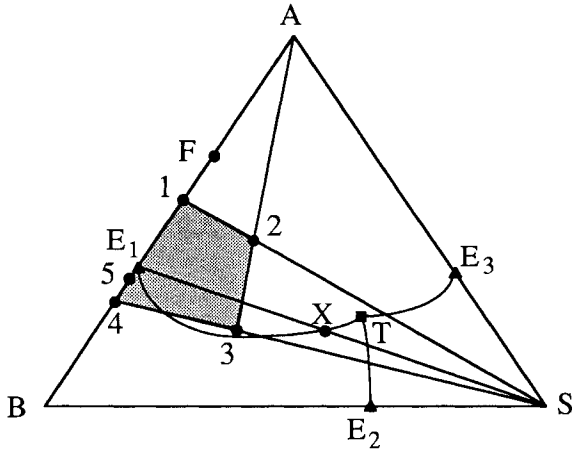

a. Type I flowsheet used for separation

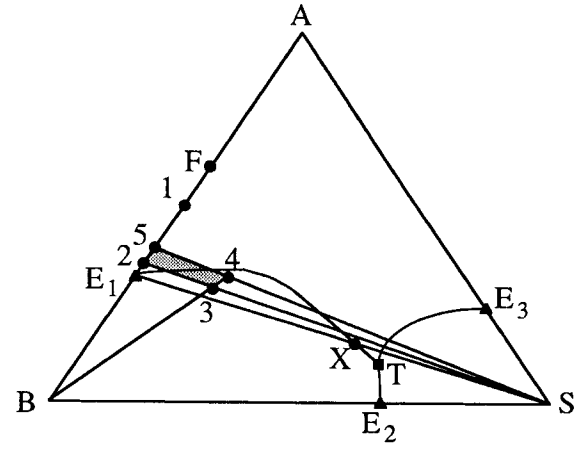

b. Type II flowsheet used for separation

Figure 5. Solid-liquid phase diagram with eutectic trough intersected by E_1S.

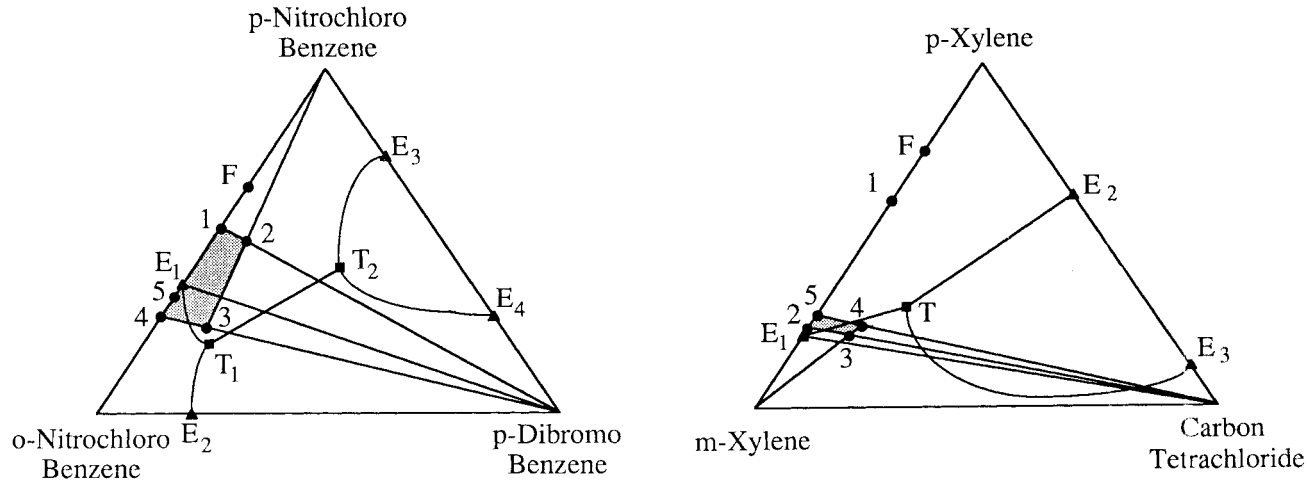

a. *p*-Nitrochlorobenzene, *o*-nitrochlorobenzene, *p*-dibromobenzene system

b. *p*-Xylene, *m*-xylene, carbon tetrachloride system

Figure 6. Solid-liquid phase diagrams.

Design Equations and Constraints

It can be seen from the preceding material that the important element in the design of extractive crystallization processes is the solid-liquid phase diagram. Wolten and Wolcox (1967) provide a discussion of the various types of phase diagrams. Solid-liquid phase diagrams can be obtained by experiments and/or theoretical predictions. A comprehensive review of the experimental techniques for the determination of solubility is available (Zimmerman, 1952). Theoretical prediction of solubility, in terms of liquid phase composition, is often based on the following standard equation (Prausnitz et al., 1986):

$$\ln \frac{1}{\gamma_i x_i} = \frac{\Delta H_i^f}{RT_{ti}}\left(\frac{T_{ti}}{T} - 1\right) - \frac{\Delta C_{pi}}{R}\left(\frac{T_{ti}}{T} - 1\right) + \frac{\Delta C_{pi}}{R} \ln \frac{T_{ti}}{T} \quad (1)$$

The various predictive methods for the activity coefficient have been summarized by Moyers and Rousseau (1987). For instance, Gmehling et al. (1978) used UNIFAC for predicting liquid phase activity coefficients and to calculate the solid-liquid equilibria for a variety of systems and compared them with experimental results. Walas (1985) describes a simple procedure to develop the solid-liquid phase diagram for a three-component system using Eq. 1. It seems that the predictions for systems with compound formation are still not yet reliable. Therefore, we recommend that experimental verification of the solid-liquid phase diagram predicted by models be an integral step in flowsheet development.

After identifying the solid-liquid phase diagram for the system, the next step in flowsheet development is to select the two crystallizer temperatures. To avoid eutectic crystallization, that is, co-crystallization of the components, the crystallizer temperatures are constrained by the solid-liquid phase relationship. The constraints on the temperatures of the crystallizers and the design equations for the two flowsheet types are given below. The discussion is intended for the case where the activity coefficient in Eq. 1 is unity. The approach to the general case of nonideal solutions is the same except that iterations are required in the solution of the equations.

Type I

The crystallizer temperature constraints are given in Eqs. 2 and 3. The first crystallizer temperature is chosen to be less than the binary eutectic temperature since it is close to the eutectic trough E_1T, and has to be higher than the ternary eutectic temperature. The exact value depends on the position of point *3* in Figure 1.

$$T_{E1} > T_{C1} > T_T \quad (2)$$

Since solvent is not present in the second crystallizer, the second crystallizer temperature must lie along side AB of the ternary diagram. The exact value depends on the position of point *5* in Figure 1. It has to be higher than the binary eutectic temperature to avoid eutectic crystallization and has to be lower than the melting point of B.

$$T_{mB} > T_{C2} > T_{E1} \quad (3)$$

Thus, the two crystallizer temperatures are design variables. According to Eq. 1, once we fix crystallizer *1* temperature, T_{C1}, the composition of A at the first crystallizer, x_{A1}, is also fixed if we assume that the activity coefficient is a constant. This implies that point *3* in Figure 7 must lie along the horizontal T_{C1} isotherm, which is shown as a dashed line KL. In the case in which the activity coefficient is not a constant, KL is actually a curve. Point *3* has to be fixed by choosing a third design variable such as x_{B1}, which is constrained within a certain range. When point *3* is very close to the eutectic trough, E_1T, we get the maximum value of x_{B1}. This corresponds to point K, the saturation concentration of B at T_{C1} and it can be calculated from Eq. 1. It turns out that the minimum value for x_{B1} corresponds to the point L, where the line KL intersects the line $5S$. We will prove this claim after deriving Eq. 10. Obviously, the composition of the solvent, x_{S1}, is also fixed after we fix T_{C1} and x_{B1}. On the contrary, point *5* is fixed once crystallizer *2* temperature, T_{C2}, is selected. Since point *5* lies

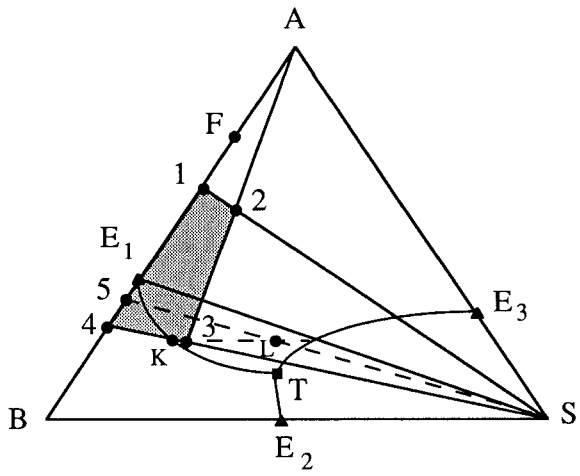

Figure 7. Feasible range of variation for the value of x_{B1}.

along the edge AB of the ternary diagram, the compositions of components A and B, x_{A2} and x_{B2}, are also fixed.

We are now ready to derive the equations for the recycle flow rates. Let us start at stream *3* in Figure 2. The molar flow rate for component B in stream *3* must be equal to (F_B+R_B), the sum of the feed and recycle flows for B. This is because B is not removed from the first crystallizer-filter system. The total molar flow rate of stream *3* is obviously equal to $(F_B+R_B)/x_{B1}$. The corresponding molar flow rate of component A is $(F_B+R_B)x_{A1}/x_{B1}$. Since there is neither addition nor removal of A between streams *3* and *5*, the recycle molar flow rate for A, indicated in Figure 2, is

$$R_A=(F_B+R_B)\frac{x_{A1}}{x_{B1}} \tag{4}$$

Based on similar arguments, we can obtain the expression for the recycle flow rate for B as

$$R_B=R_A\frac{x_{B2}}{x_{A2}} \tag{5}$$

The composition of B in the liquid phase, x_{B2}, can be obtained from Eq. 1 if we assume that the activity coefficient is a constant, because the second crystallizer temperature, T_{C2}, is already fixed. Substituting Eq. 5 into Eq. 4 and solving for R_A, and noting that the composition of A in the second crystallizer, x_{A2}, is equal to $(1-x_{B2})$, we get

$$R_A=\frac{F_B}{\left[\frac{x_{B1}}{x_{A1}}-\frac{x_{B2}}{(1-x_{B2})}\right]} \tag{6}$$

Thus, R_B can be determined from Eq. 5 after calculating R_A in Eq. 6. Returning to stream *3*, we can easily see that the recycle solvent flow rate is given by

$$R_S=R_A\frac{(1-x_{A1}-x_{B1})}{x_{A1}} \tag{7}$$

The feed flow rates to the crystallizers can be derived by using simple material balances and are given in Eqs. 8 and 9.

$$F_{C1}=F+R_A+R_B+R_S \tag{8}$$

$$F_{C2}=F_{C1}-F_A-R_S \tag{9}$$

By inspection of Eq. 6, we can see that to avoid infinite flow rates or negative recycle flow rates, an additional constraint needs to be satisfied:

$$\frac{x_{B1}}{x_{A1}}-\frac{x_{B2}}{(1-x_{B2})}>0 \tag{10}$$

The above constraint also implies a lower bound for x_{B1}. After fixing T_{C2}, the line *5S* in Figure 7 is fixed. From elementary trigonometry, any point above the line *5S* would violate the inequality in Eq. 10. Thus, the minimum value of x_{B1} corresponds to point L in Figure 7. The impact of choosing x_{B1}, away from the eutectic trough, on the recycle and the solvent flows will be analyzed in a case study of *para* and *meta* xylenes.

Type II

Similarly, we can identify the constraints on the crystallizer temperatures and develop the recycle material balances for type II. The corresponding equations are given in Table 1.

The important design variables in this process are the two crystallizer temperatures and the mole fraction of B at crys-

Table 1. Constraints and Material Balance Equations for Type II Flowsheet.

Crystallizer Temperature Constraints

$$T_{mA}>T_{C1}>T_{E1} \tag{11}$$

$$T_{E1}>T_{C2}>T_T \tag{12}$$

Recycle Flow Rates

$$R_A=\frac{F_B}{\left(\frac{1-x_{A1}}{x_{A1}}\right)-\frac{x_{B2}}{x_{A2}}} \tag{13}$$

$$R_B=R_A\frac{x_{B2}}{x_{A2}} \tag{14}$$

$$R_S=R_A\frac{(1-x_{A2}-x_{B2})}{x_{A2}} \tag{15}$$

Feed Flow Rates

$$F_{C1}=F+R_A+R_B \tag{16}$$

$$F_{C2}=F_{C1}-F_A+R_S \tag{17}$$

Additional Constraint

$$\left(\frac{1-x_{A1}}{x_{A1}}\right)-\frac{x_{B2}}{x_{A2}}>0 \tag{18}$$

tallizer *1*. However, if we locate point *3* very close to the eutectic trough E_1T, we can calculate the molar composition of *B* in the liquid phase from Eq. 1 if we assume an activity coefficient of unity. For this special case, not only is x_{A1} a function of T_{C1}, but x_{B1} is also a function of T_{C1}. Some interesting analytical solutions can be obtained for this limiting case. For example, the solvent flow rate in the type I flowsheet can be minimized with respect to the first crystallizer temperature by solving the equation $dR_S/dT_{C1}=0$. Substitution of R_S from Eqs. 7 and 6 leads to

$$\frac{d}{dT_{C1}}\left[\frac{F_B(1-x_{A1}-x_{B1})}{x_{B1}-\dfrac{x_{A1}x_{B2}}{(1-x_{B2})}}\right]=0 \qquad (19)$$

Carrying out the differentiation of Eq. 19 for this limiting case, we get after simplification with Eq. 1

$$\Delta H^f_A x_{A1}\left[(1-x_{B1})\frac{x_{B2}}{(1-x_{B2})}-x_{B1}\right] - \Delta H^f_B x_{B1}\left[1-x_{A1}-\left(\frac{x_{B2}}{1-x_{B2}}\right)x_{A1}\right]=0 \qquad (20)$$

Equation 20 represents the condition under which the recycled solvent flow rate is a minimum for a given temperature of the second crystallizer. It is useful for checking numerical schemes and for obtaining quick answers.

Process Economic Trade-offs

The general extractive crystallization procedure can be better understood by examining an example process flowsheet for separating *para*-xylene from *meta*-xylene. The extractive solvent used in this process is *n*-pentane. The solid-liquid phase diagram for this system is shown in Figure 8. As in Figures 6a and 6b, the relative positions of the eutectics are correctly indicated but are not very exact. Note that the ternary eutectic *T* is very close to the binary eutectic E_2. We can identify from the solid-liquid phase diagram that this system falls into type I and the flowsheet in Figure 2 can be used for separating the two components. In this case, *para*-xylene corresponds to component *A* and *meta*-xylene to component *B* in Figure 2. Most of the physical properties needed for the calculations can be obtained from various sources (Mullin, 1972; Dale, 1981; Reid et al., 1987). The parameters for the crystallization kinetics (Garside and Shah, 1980) are estimated values. A summary of the various design variables and process data used in the calculations is given in Table 2.

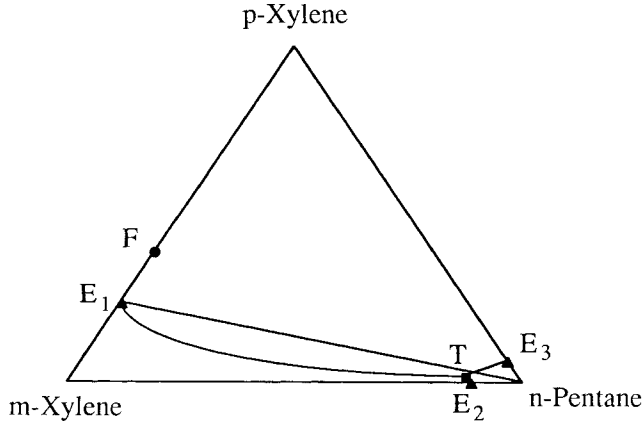

Figure 8. Solid-liquid phase diagram for *p*-xylene, *m*-xylene, *n*-pentane system.

Table 2. Values of Some Input Parameters for Xylenes Plant

Production Rate, ton/yr *p*-xylene	40,000
Feed Composition, mol frac.	
p-xylene	0.333
m-xylene	0.667
Melting Point, °C	
p-xylene	13.3
m-xylene	− 47.9
n-pentane	− 129.7
Eutectic Temp., °C	
p-, *m*-xylenes	− 52.56
m-xylene, *n*-pentane	− 130.44
p-xylene, *n*-pentane	− 129.89
Ternary eutectic	− 130.50
Enthalpy of Fusion, kJ/kmol	
p-xylene	17,100
m-xylene	11,570
n-pentane	8,395
Crystallizer Temp., °C	
Precrystallizer	− 51
Crystallizer 1	− 90
Crystallizer 2	− 51
Crystallization Kinetics	
p-xylene	$i=1.5$, $=0.5$ $k_r=1.0\times10^{20}$
m-xylene	$i=1.5$, $=0.5$ $k_r=1.0\times10^{20}$
Filter Parameters	
Rotation speed	0.5 rpm
Submergence	120°
Vacuum level	35,000 N/m^2
Porosity	0.4

In the following, we assume that point *3* in Figure 7 is very close to the eutectic trough E_1T. Thus, the only important design variables are the two crystallizer temperatures. The feasible region of operation for both crystallizers is shown Figure 9. The horizontal line of the feasible region corresponds to the temperature of the binary eutectic between *para* and *meta* xylenes, − 52.56°C. According to Eq. 3, T_{C2} must be higher than this temperature. The curved line of the feasible region is calculated with Eq. 10 by setting the lefthand side of the equation to zero. If the two crystallizer temperatures are chosen to lie on this curve, infinite flow rates of the solvent and the recycled xylenes are required to obtain pure products. The use of crystallizer temperatures above the feasible region would lead to practically impossible negative flow rates, as can be seen in Eqs. 5 to 7.

The influence of the first crystallizer temperature, T_{C1}, on the solvent flow rate and the xylenes recycle flow rate is given in Figure 10, for which T_{C2} is fixed at the base case value of − 51°C. We can see that there is an optimum temperature at

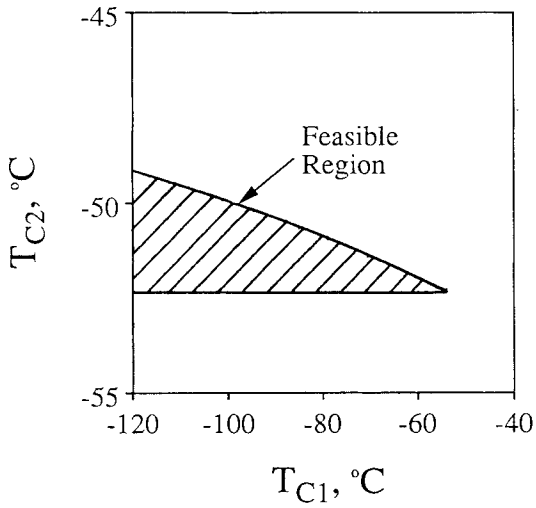

Figure 9. Feasible region of operation for crystallizer temperatures.

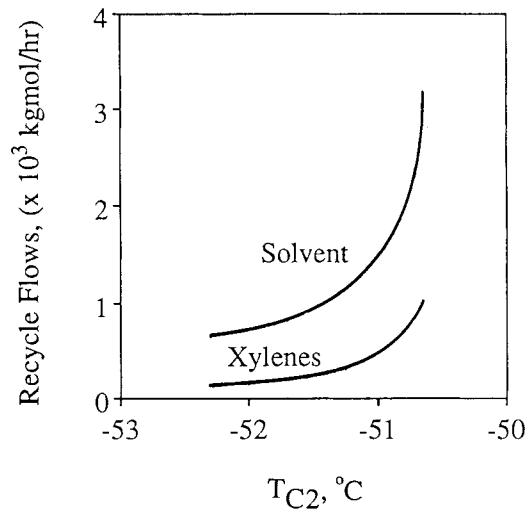

Figure 11. Dependence of recycled solvent and recycled xylenes flow rates on second crystallizer temperature.

which the solvent flow rate is a minimum and that the recycled xylenes flow rate decreases with crystallizer *1* temperature. Note that x_{A1} and x_{B1} are both functions of T_{C1} and Eq. 20 can be solved for the optimal T_{C1} for different values of T_{C2}. The optimal value of T_{C1} obtained in this way is about -94.7°C, which is very close to the value we get from the graph in Figure 10.

The solvent flow rate and the recycle flow rates of the xylenes are also influenced by the second crystallizer temperature. This is illustrated in Figure 11, for which T_{C1} is fixed at the base case value of -90°C. Both flow rates decrease with a decrease in the second crystallizer temperature.

In Figure 12, the influence of T_{C2} on the optimal T_{C1} and the corresponding total recycle flow rate $(R_p+R_m+R_S)$ are shown. We find that as the second crystallizer temperature decreases to the value of the eutectic temperature, T_{E1}, of -52.56°C, the optimal T_{C1} increases and the total recycle flow rate decreases. This would lead to lower equipment costs, such as that for the refrigeration compressor. One might conclude that it is always better to operate the second crystallizer as close to the eutectic point as possible. It should be emphasized however that purity considerations, such as the possibility of mother liquor occlusion in the crystals, have not been included here and need to be taken into account while deciding the crystallizer temperature.

The mole fraction of *B* at crystallizer *1*, x_{B1}, becomes a new design variable when we relax the assumption that point *3* in Figure 7 is very close to the eutectic trough E_1T. We can change x_{B1} over the constrained range between points *K* and *L*. The minimum value of x_{B1} is obtained by rearranging Eq. 10:

$$x_{B1} > x_{A1}\left(\frac{x_{B2}}{x_{A2}}\right) \tag{21}$$

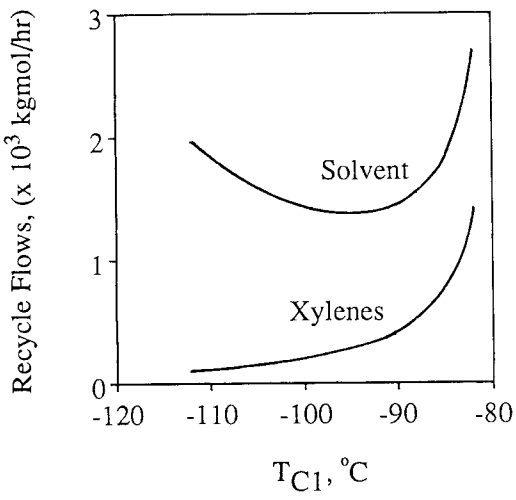

Figure 10. Dependence of recycled solvent and recycled xylenes flow rates on first crystallizer temperature.

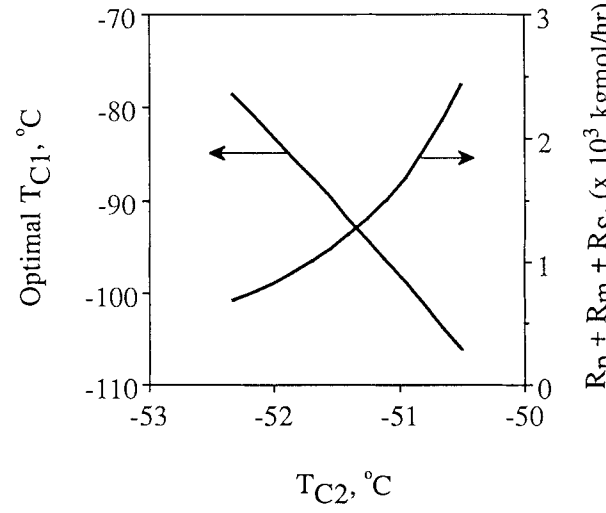

Figure 12. Dependence of optimal first crystallizer temperature and minimum total recycle flow rate on second crystallizer temperature.

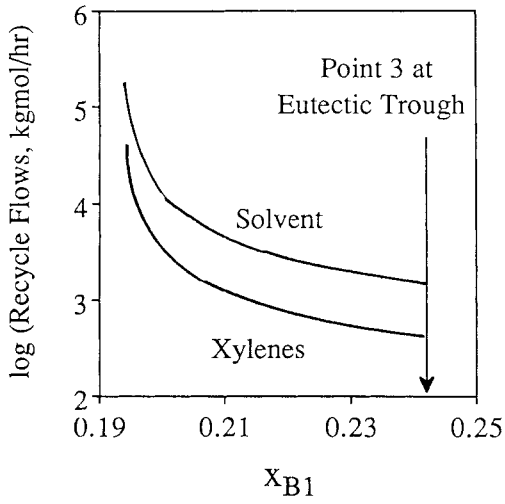

Figure 13. Dependence of recycled solvent and recycled xylenes flow rates on x_{B1}.

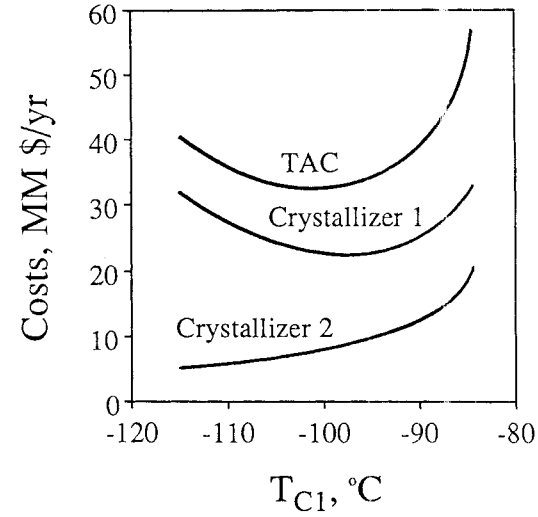

Figure 14. Dependence of total annualized cost, first crystallizer cost, and second crystallizer cost on first crystallizer temperature.

The maximum value of x_{B1} is the value corresponding to the condition that point *3* is very close to the eutectic trough, E_1T. The xylenes and the solvent recycle flow rates needed for complete separation for various values of x_{B1} are determined. The impact of the value of x_{B1} on the recycle flow rates of the xylenes and the solvent is shown in Figure 13. The recycle flow rates are the lowest when point *3* is very close to the eutectic trough, E_1T, and would lead to lower equipment and operating costs. Again, this analysis does not include any purity considerations and these need to be accounted for during detailed design.

Equipment design models for MSMPR crystallizers and rotary vacuum filters are available in many standard texts (Peters and Timmerhaus, 1980; *Chemical Engineers' Handbook*, Perry and Chilton, 1973), and are not repeated here. Models for refrigeration unit design are obtained from Shelton and Grossmann (1985). The cost models for the various equipment have been obtained from Walas (1988) and Happel and Jordan (1975), and current costs are estimated with the Marshall and Swift index.

The impact of the first and second crystallizer temperatures on the overall process economics is shown in Figures 14 and 15. A capital charge factor of one-third per year is used to annualize capital costs. The total annualized cost and the two crystallizer systems costs, which include the crystallizer costs and the refrigeration unit costs, are plotted against the first crystallizer temperature, T_{C1}, in Figure 14. Again, T_{C2} is fixed at the base case value of -51°C. The optimum first crystallizer temperature is about -101°C, at which the total annualized cost shows a minimum. The first crystallizer system cost decreases with decreasing crystallizer temperature initially, due to the reduction in solvent and recycle flow rates, Figure 10. However, the solvent flow rate increases upon further decrease in T_{C1}. Also, the refrigeration unit cost increases with decreasing crystallizer temperature. Therefore, we see an optimum for the first crystallizer system cost. The second crystallizer system cost decreases monotonically with decreasing T_{C1} because of a reduction in the recycled xylenes flow rate.

The influence of the second crystallizer temperature, T_{C2}, on the total annualized cost and the two crystallizer systems costs is illustrated in Figure 15. Again, T_{C1} is fixed at the base case value of -90°C. The total annualized cost decreases with decreasing second crystallizer temperature. The range of the second crystallizer temperature is constrained to a narrow region of about 1°C as dictated by Eqs. 3 and 10. It is important to note that the total annualized cost is very sensitive to small changes in the second crystallizer temperature.

Comparison of General Methodology with Conventional Procedure

The general extractive crystallization procedure can be compared with the conventional procedure by examining an existing process flowsheet for separating the same system of components. The conventional process flowsheet, as given by Findlay and Weedman (1958) and Dale (1981), is shown in

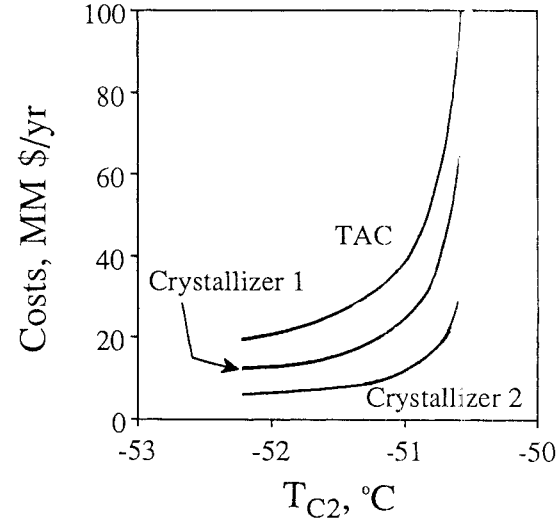

Figure 15. Dependence of total annualized cost, first crystallizer cost, and second crystallizer cost on second crystallizer temperature.

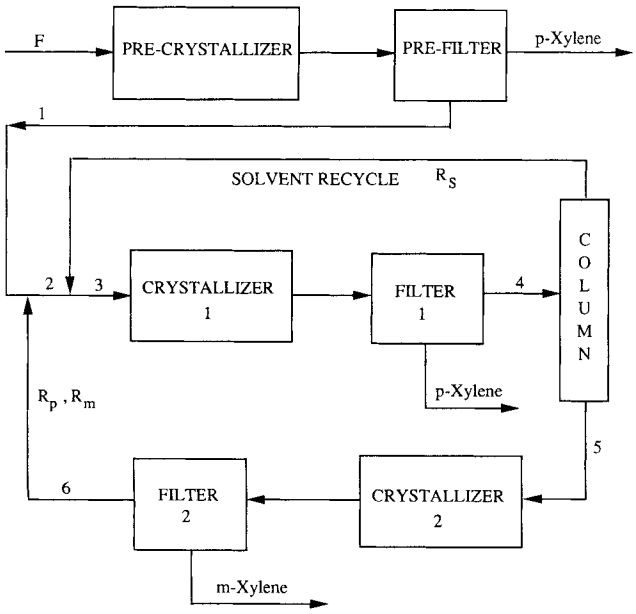

Figure 16. Conventional process flowsheet for separating xylene isomers.

Figure 16. Three crystallizers and three filters are needed for this separation scheme. The appropriate solid-liquid phase diagram with the relevant compositional markings is shown in Figure 17.

The feed stream is represented by point F in the phase diagram, Figure 17, and is fed to the precrystallizer, where the temperature is maintained at T_{CP}. *Para*-xylene is crystallized from the feed and is separated from the mother liquor in the prefilter. The composition of the mother liquor from the precrystallizer moves down to point *1* in the phase diagram. The recycled *para*-xylene and *meta*-xylene mixture from the second crystallizer with composition represented by *6* is added to this stream. The composition of the mixed stream is represented by point *2* in the phase diagram. The recycled solvent from the solvent recovery column is added to this new stream. The mixed stream with composition represented by point *3* is fed to the first crystallizer. The temperature of the first crystallizer

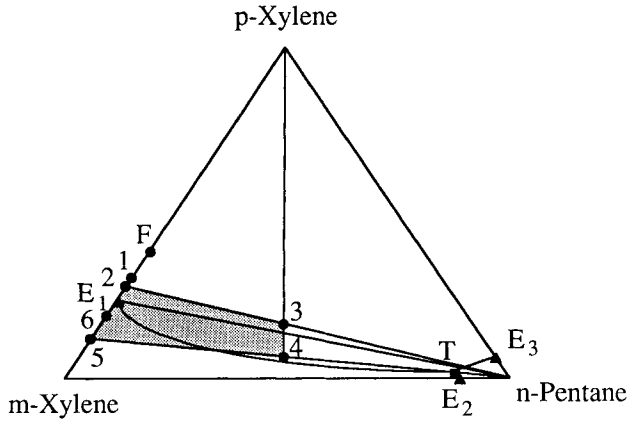

Figure 17. Solid-liquid phase diagram for *p*-xylene, *m*-xylene, *n*-pentane system with compositional markings for conventional process flowsheet.

Table 3. Constraints and Material Balance Equations for Conventional Procedure

Crystallizer Temperature Constraints

$$T_{mp} > T_{CP} > T_{E1} \tag{22}$$

$$T_{CP} > T_{C1} > T_T \tag{23}$$

$$T_{mm} > T_{C2} > T_{E1} \tag{24}$$

Recycle Flow Rates

$$R_p = \frac{F_m}{\left[\frac{x_{m1}}{x_{p1}} - \frac{x_{m2}}{(1-x_{m2})}\right]} \tag{25}$$

$$R_m = R_p \frac{x_{m2}}{(1-x_{m2})} \tag{26}$$

$$R_S = R_p \frac{(1-x_{p1}-x_{m1})}{x_{p1}} \tag{27}$$

Feed Flow Rates

$$F_{CP} = F \tag{28}$$

$$P_{pP} = F_p - \left(\frac{F_m x_{pP}}{1-x_{pP}}\right) \tag{29}$$

$$F_{C1} = F + R_p + R_m + R_S - P_{pP} \tag{30}$$

$$F_{C2} = F_{CP} - F_p + R_p + R_m \tag{31}$$

Additional Constraint

$$\frac{x_{m1}}{x_{p1}} - \frac{x_{m2}}{(1-x_{m2})} > 0 \tag{32}$$

is maintained at T_{C1}, and more *para*-xylene is crystallized from the solution. The mother liquor composition moves further down to point *4* in the phase diagram. The crystals are separated from the mother liquor in filter *1*. The mother liquor is fed to the solvent recovery column, where the solvent is separated and recycled to the first crystallizer feed. The column bottoms with composition *5* is fed to the second crystallizer. The second crystallizer temperature is maintained at T_{C2} and *meta*-xylene is crystallized from the solution. The *meta*-xylene crystals are separated from the mother liquor in filter *2*. The mother liquor, whose composition is represented by point *6*, is recycled to the first crystallizer feed stream.

The constraints on the crystallizer temperatures and the relationships between the recycle flow rates of the xylenes and the solvent, and crystallizer temperatures, can be similarly derived and are given in Table 3.

The process flowsheet scheme can be compared with the general methodology by finding the cost of individual equipment and the associated operating cost, Table 4. The costs for the refrigeration compressor, the condenser, and the reboiler include both capital and operating costs. The total annualized cost of the general procedure is however only about 3% less than that of the conventional procedure.

Table 4. Equipment Cost Comparison of Conventional and General Procedures

Equipment Item	Cost, MM $/yr Conventional Proc.	General Proc.
Precrystallizer	0.697	-
Heat exchanger	0.821	-
Refrigeration compressor	0.691	-
Crystallizer 1	0.703	1.247
Heat exchanger 1	12.03	12.22
Refrigeration compressor 1	10.45	10.62
Solvent recovery column	0.216	0.215
Condenser	0.907	0.907
Reboiler	1.252	1.242
Crystallizer 2	1.173	1.173
Heat exchanger 2	5.767	5.767
Refrigeration compressor 2	4.975	4.975
Prefilter	0.035	-
Filter 1	0.020	0.043
Filter 2	0.067	0.067
Total cost	39.804	38.476

Conclusions

The procedure for separating a binary system by means of extractive crystallization has been generalized so that it can be applied for a given chemical system in a systematic manner. We propose two different flowsheet structures for separating components with different solid-liquid phase behaviors. Design equations for these flowsheet structures have been formulated. They are expected to be useful in conceptual design in which the interconnections among units in a process are to be fixed (Douglas, 1988; Rajagopal et al., 1988). Design constraints have also been identified. For example, the crystallizer temperatures of the extractive crystallization process are confined within a feasible region of operation, Figure 9. In addition, the important design variables in the process are identified and their relative economic impact on the process are quantified in an example—the separation of *para*-xylene from *meta*-xylene with *n*-pentane as the extractive solvent. We conclude that the recycled solvent flow rate can be minimized with respect to the first crystallizer temperature. The second crystallizer temperature should be chosen such that the composition of the resulting mother liquor is close to the eutectic point between *para* and *meta* xylenes. Similarly, the mother liquor composition at the exit of the first crystallizer should be chosen to be close to the eutectic trough emanating from the same eutectic point.

The present study is still limited in scope. For instance, if one operates a crystallizer too close to a eutectic point or eutectic trough, cocrystallization might occur because, in reality, the temperature in a crystallizer cannot be perfectly uniform. We have not included any consideration for high growth rates and the associated problem of mother liquor occlusion in the crystals. Therefore, the suggestions regarding the selection of crystallizer temperatures must be relaxed accordingly, based on the experience of the crystallization experts. We considered only a single theoretical stage for crystallization, as predicted by thermodynamics. In practice, more than one stage would be needed for obtaining pure crystalline products.

Finally, we emphasize the relevance of this study to process design. Extractive crystallization usually does not exist alone. In the disproportionation of toluene, for example, toluene reacts with hydrogen to form benzene, and *ortho*, *para*, and *meta* xylenes, among other minor components. Benzene, toluene and *ortho*-xylene are first removed by using distillation. The *para* and *meta* xylenes can then be separated by extractive crystallization. Therefore, extractive crystallization is a subsystem of a much larger plant. We have not considered the potential interactions, such as heat integration and solvent movement, between this subsystem and the rest of the complete plant. In fact, there are many other alternatives, such as the use of molecular sieves to favor the formation of one isomer over the others, and the recycle of *meta*-xylene to an isomerization reactor to make more *para*-xylene. The value of our general methodology for the extractive crystallization of a binary mixture should be considered as a useful tool for evaluating process alternatives rather than an end in itself. That is why so much emphasis is placed on economic trade-offs in this study.

Acknowledgment

We express our appreciation to the National Science Foundation, Grant No. CTS-8821793, for support of this research.

Notation

F = feed rate, kmol/h
i = crystallization kinetics parameter
j = crystallization kinetics parameter
k_r = rate constant for crystallization, no./ [m^3s $(kg/m^3)^j$ $(m/s)^i$]
R = gas constant, J/kmol/K, Eq. 1
R = recycle flow rate, kmol/h
T = temperature, °C
x = liquid mole fraction

Greek Letters

γ = liquid phase activity coefficient
ΔC_p = heat capacity difference, J/kmol/K
ΔH = enthalpy of fusion, J/kmol

Subscripts

A,B = components to be separated
C = crystallizer
$E1,E2,E3$ = binary eutectic points
i = components
m = *m*-xylene
m = melting
p = *p*-xylene
P = precrystallizer
S = solvent
t = triple point
T = ternary eutectic point
1,2 = crystallizer number

Superscript

f = fusion

Literature Cited

Brenken, H., and F. Richter, "Urea Dewaxing Expands Feed Choice," *Hydrocarb. Process.*, 127, (Jan. 1979).

Chivate, M. R., and S. M. Shah, "Separation of *m*-Cresol and *p*-Cresol by Extractive Crystallization," *Chem. Eng. Sci.*, **5**, 232 (1956).
Dale, G. H., "Crystallization, Extractive and Adductive," *Encyc. Chem. Process Des.*, **13**, 456 (1981).
Dikshit, R. C., and M. R. Chivate, "Separation of *Ortho*-and *Para*-Nitrochlorobenzenes by Extractive Crystallization," *Chem. Eng. Sci.*, **25**, 311 (1970).
Douglas, J. M., *Conceptual Design of Chemical Processes*, McGraw-Hill, New York (1988).
Egan, C. J., and Luthy, R. V., "Separation of Xylenes," *Ind. Eng. Chem.*, **47**, 250 (1955).
Findlay, R. A., "Adductive Crystallization," *New Chemical Engineering Separation Techniques*, H. M. Schoen, ed., Interscience, New York, 257 (1962).
Findlay, R. A., and J. A. Weedman, "Separation and Purification by Crystallization," *Advances in Petroleum Chemistry and Refining*, K. A. Kobe, J. A. McKetta, eds., Interscience, New York, **1**, 119 (1958).
Garside, J., and M. B. Shah, "Crystallization Kinetics from MSMPR Crystallizers," *Ind. Eng. Chem. Process Des. Dev.*, **19**, 509 (1980).
Gmehling, J. G., T. F. Anderson, and J. M. Prausnitz, "Solid-Liquid Equilibria Using UNIFAC," *Ind. Eng. Chem. Fundam.*, **17**, 269 (1978).
Happel, J., and D. G. Jordan, *Chemical Process Economics*, Dekker, New York (1975).
McCandless, F. P., R. D. Mountain, R. D. Olson, S. P. Roth, and L. J. van Dyke, "Separation of Trimethylpentanes by Extractive Crystallization with Thiourea," *Ind. Eng. Chem. Prod. Res. Dev.*, **11**, 463 (1972).
McCandless, F. P., R. E. Cline, and M. O. Cloninger, "Separation of the Xylenes and Ethylbenzene by Extractive Crystallization with Thiourea," *Ind. Eng. Chem. Prod. Res. Dev.*, **13**, 214 (1974).
Moyers, C. G., and R. W. Rousseau, "Crystallization Operations," *Handbook of Separation Process Technology*, R. W. Rousseau, ed., Wiley, New York, 578 (1987).
Mullin, J. W., *Crystallization*, 2d ed., Butterworth, London (1972).
Perry, R. H., and C. H. Chilton, eds. *Chemical Engineers' Handbook*, 5th ed., McGraw-Hill, New York (1973).
Peters, M. S., and K. D. Timmerhaus, *Plant Design and Economics for Chemical Engineers*, 3d ed., McGraw-Hill, New York (1980).
Prausnitz, J. M., R. N. Lichtenthaler, and E. G. Azevado, *Molecular Thermodynamics of Fluid-Phase Equilibria*, Prentice-Hall, Englewood Cliffs, NJ (1986).
Rajagopal, S., K. M. Ng, and J. M. Douglas, "Design of Solids Processes; Production of Potash," *Ind. Eng. Chem. Res.*, **27**, 2071 (1988).
Reid, R. C., J. M. Prausnitz, and B. E. Poling, *The Properties of Gases and Liquids*, 4th ed., McGraw-Hill, New York (1987).
Shelton, M. R., and I. E. Grossmann, "A Shortcut Procedure for Refrigeration Systems," *Comp. Chem. Eng.*, **9**, 615 (1985).
Tare, J. P., and M. R. Chivate, "Separation of Close Boiling Isomers by Adductive and Extractive Crystallization," *AIChE Symp. Ser.*, **153**, 95 (1976).
Walas, S. M., *Phase Equilibria in Chemical Engineering*, Butterworth, Boston (1985).
Walas, S. M., *Chemical Process Equipment—Selection and Design*, Butterworth, Boston (1988).
Wolten, G. M., and W. R. Wilcox, "Phase Diagrams," *Fractional Solidification*, M. Zief, W. R. Wilcox, eds., Dekker, New York, **1**, 21 (1967).
Zimmerman, H. K., "The Experimental Determination of Solubilities," *Chem. Rev.*, **51**, 25 (1952).

Manuscript received June 19, 1990, and revision received Jan. 17, 1991.